LA-UR-09- 10-01376

Approved for public release; distribution is unlimited.

Title: ELECTROMAGNETIC EFFECTS ON EXPLOSIVE REACTION AND PLASMA

Author(s): Douglas G. Tasker, Von H. Whitley, Jonathan L. Mace, Steven J. Pemberton, Thomas D. Sandoval and Richard J. Lee

Intended for: Proceedings of 14th International Detonation Symposium, Coeur d'Alene, Idaho, April 11 to 16, 2010

Los Alamos
NATIONAL LABORATORY
EST. 1943

Electromagnetic Effects on Explosive Reaction and Plasma

Douglas G. Tasker*, Von H. Whitley*, Jonathan L. Mace*,
Steven J. Pemberton*, Thomas D. Sandoval* and Richard J. Lee[†]

*DE-division, Los Alamos National Laboratory
Los Alamos, NM 87545, USA

[†]Indian Head Division,
Naval Surface Warfare Center, Indian Head, MD 20640, USA

Abstract. A number of studies have reported that electric fields can have quantifiable effects on the initiation and growth of detonation, yet the mechanisms of these effects are not clear. Candidates include Joule heating of the reaction zone, perturbations to the activation energy for chemical reaction, reduction of the Peierls energy barrier that facilitates dislocation motion,[1] and acceleration of plasma projected from the reaction zone. In this study the possible role of plasma in the initiation and growth of explosive reaction is investigated. The effects of magnetic and electric field effects on reaction growth will be reviewed and recent experiments reported.

Introduction

Possible Role of Plasma in Explosive Reaction

Plasma ejected from reacting explosives have been studied extensively[2-7] yet their role in the initiation and propagation of detonation remains unclear. The luminous plasma observed at the free surfaces of detonating explosives have been observed travelling at velocities of ~20 km/s in a partial vacuum of ~1.3 Pa with densities estimated to be up to 70 kg/m^3 but typically <1 kg/m^3.[6,8] Moreover, plasma temperatures of 10,000 to 20,000 K have been estimated. As these plasma are present at the free surfaces of reacting explosives they must also be present within the interstices of reacting granular explosives and impact downstream unreacted explosive crystals. If explosively-generated plasma do play a role in the initiation and growth of reaction, or detonation, it may be possible to control the process by the application of electric fields, thereby modifying explosive sensitivity and performance.

Data from various experiments performed at the Los Alamos National laboratory (LANL) are reported where plasma were projected into cylindrical guides from detonating charges of PBX-9501 and their progress was measured by high speed framing photography, X-ray and proton radiography,[9] and Photon Doppler Velocimetry (PDV).[10] In one series of experiments the plasma were subjected to 1-Tesla magnetic fields and in another series the plasma were subjected to longitudinal electric fields with potential differences of up to ±60 kV. In other experiments, wedges of PBX-9502 were subjected to transverse electric fields to determine their effects on detonation failure.

The effect of 1-T magnetic fields on the initiation and growth of explosives was also studied in the Modified Gap Test (MGT) in experiments similar to those performed by Lee with magnetic fields.[11]

Electric Field Effects on Explosives

Cook[12] reported that the application of a parallel[a] electric field caused significant changes to the run distance to detonation in explosive Comp-B. In similar experiments Lee[13] studied the effects of electric fields on the initiation and growth of reaction in an HMX-based cast-cured explosive using the modified gap test (MGT) and observed modest effects.

Detonation failure study in electric field

In experiments performed at the Atomic Weapons Establishment (AWE) in England by Salisbury and Winter,[14,15] it was shown that transverse electric fields could significantly affect the failure thickness of TATB-based explosive EDC-35. The thickness of the plane wedges of EDC-35 varied from 6 mm to 1 mm along a 100-mm length, i.e., they had a 3° taper. Each wedge was initiated across its 50-mm width by a line wave generator at its thickest edge and the progress of the detonation was observed by streak camera. Aluminum electrodes were placed above and below the wedges and a 4-μF or 16-μF capacitor charged to 25 kV was discharged through the detonating explosive. The detonation would fail at a critical failure thickness and the effect of the electric field on that failure thickness was observed by steak camera.

We will describe similar experiments on another TATB-based explosive that supported these observations.

Possible explanations for electric field effect

Possible explanations for these electric field effects include: bulk heating of the reaction products by Joule heating; reduction of the energy barrier that facilitates dislocation motion, perturbations to the activation energy for chemical reaction, and acceleration of plasma projected from the reaction zone.

[a] Parallel and transverse are parallel and perpendicular to the detonation velocity vector.

In this study the possible role of plasma in the initiation and growth of explosive reaction and detonation is investigated.

Magnetic Field Effects on Explosives

Previous work

Significant magnetic effects have been reported by Cook on plasma generated by a liquid explosive Dithekite 13 (nitrobenzene/ nitric acid/ water 63/24/13, by weight) in a magnetic field of ~0.1 T.[16] Plasma generated by the detonating Dithekite was projected from a 6.4-cm diameter glass tube and entered the magnetic field. The plasma left the explosive charge at a velocity of 7.3 km/sec, entered the magnetic field at 17.0 km/sec, and then left the field at 1.3 km/sec; it also described a helical path through the field. (The strength of the field is significant because 0.1-T magnetic fields are also used to study the propagation of reaction in explosives using electromagnetic velocity (EMV) particle velocity gauges.[17] If a 0.1-T magnetic field caused these magnetic effects then the validity of EMV gauge measurements is put into question.)

Magnetic fields cannot change the kinetic energy

The Cook[16] results would not be expected because the magnetic (Lorentz) force $\boldsymbol{F}$ on a charged particle is always normal to its velocity vector and therefore cannot change its kinetic energy, γ eV. It can only change its direction, i.e., $\boldsymbol{F} = q\boldsymbol{v} \times \boldsymbol{B}$, where q is the electronic charge, $\boldsymbol{v}$ the velocity and $\boldsymbol{B}$ the field. Ejecta from the surface of a detonating charge tend to expand on a hemispherical front. It is *possible* that ionized plasma could be focused by a parallel magnetic field.

A charged particle of mass m is deflected by a magnetic field into a circle of radius r as follows

$$r = \frac{mv}{Bq} = \frac{1}{B}\sqrt{2\gamma\frac{m}{q}} \qquad (1)$$

Now $B = 0.1$ T in the Cook experiments so if the 20-km/s ejecta reported by Spaulding[8] were electrons, i.e., the least massive and therefore least energetic, then their kinetic energy γ would be

~2 eV and, given e/m_e = -1.759 x 10^{11} C/kg, r_e = 48 μm.

Also, magnetic deflections of charged particles should be overwhelmed by collision effects in air. As the Cook experiments were performed in air at 1 bar, $r_e \backslash \lambda = 210$ where λ is the mean free path between collisions ($\lambda \approx 230$ nm for an electron in air at STP).

1-T magnetic fields in LANL experiments

In the magnetic experiments performed at LANL that follow, solid explosive HMX-based explosive charges were detonated in air at ~0.78 bar within either transverse or parallel quasi-static 1-T fields. So from (1) the deflection radius r_e = 4.8 μm, and $r_e/\lambda = 16$.

Experiments in Electric Fields

Some recent work on the effects of electric and magnetic fields will be summarized. The effects of electric fields on the initiation and growth of reaction in an HMX-based cast-cured explosive using the modified gap test (MGT) were reported by Lee.[11] Similar experiments were performed by the authors to determine the effects of 1-Tesla magnetic fields on the same explosive in the MGT.

Detonation Failure Experiments in Electric Fields

The AWE study[14,15] showed that transverse electric fields can change the failure thickness of TATB-based explosive EDC-35. Similar experiments were performed at LANL to verify these results, **Error! Reference source not found.**. Streak photography was not used because it can be affected by electrical discharges along the edges of electrodes.[18] Instead, 25.4-mm thick polished witness blocks made from stainless steel 304 and ionization pins were used to detect the detonation front positions.

Two parallel wedges of explosive PBX-9502, containing 95% TATB by weight and a close equivalent to EDC-35, with densities of 1890 kg/m^3 were placed side by side on a single witness block. Each pair of wedges was machined out of a single block of explosive so their densities and compositions were nearly perfectly matched.

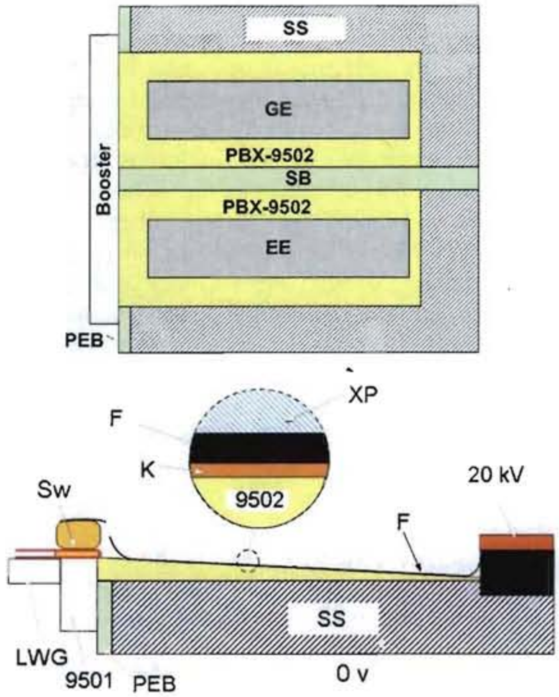

Figure 1. Schematic of the parallel wedges experiment. Top: plan view; bottom: side elevation. Key: 9502 – PBX-9502 explosive; EE - energised electrode; F – 250-μm Al. foil; GE - grounded and shorted electrode; K – 75-μm polyimide insulation; LWG – line wave generator; PEB - polyethylene barrier; SB - shock barrier; SS - stainless steel witness block; XP – expanded polystyrene.

The wedges each had a 3° taper and were 50 mm wide, with thicknesses varying from 7.92 mm to 1 mm over their lengths. They were initiated at their thick ends (the left of the figure) with a common line wave generator and PBX-9501 (95% HMX) booster explosive. A polyethylene shock barrier was used to protect the witness block from the booster system and the two wedges were separated by a polyethylene shock barrier to delay the communication of the detonation front of one wedge with that of the other. As in the AWE experiments, the 25-mm wide foil electrode was insulated from the explosive with a 75-μm layer of polyimide insulation[19] to prevent premature breakdown of the explosive. The foil and polyimide were gently pressed against the explosive to ensure good electrical contact with a layer of expanded polystyrene.

The top electrode of one wedge was connected to a 20-kV, 300-μF, 60-kJ capacitor bank. This was named the *Hot* electrode, whereas the top electrode of the other wedge was electrically short-circuited to the bottom ground electrode and called the *Control*; otherwise their assemblies were identical. Ionization pins were placed in the grounded witness block to detect the positions of the detonation fronts with time. Contactless (inductive) techniques were used measure electrical currents and voltages without creating ground loops. In this way it was verified that the voltage on the Control side remained at zero, i.e., there was no arcing across from the Hot side. Currents were measured with current transformers[20] and voltages were measured with copper sulfate voltage probes.[21] (The switches on the left in Figure 1 protected the voltage probes from prolonged exposure to the applied voltages.)

Results of Parallel Wedge Experiments

Experiments were performed with the capacitor bank power supply charged to voltages between 10 kV and 18 kV. It was found that up to 15 kV there was no apparent difference between the results, either in the ionization pin or witness block data. However, at a charge voltage of 18 kV differences were observed as in Figure 2.

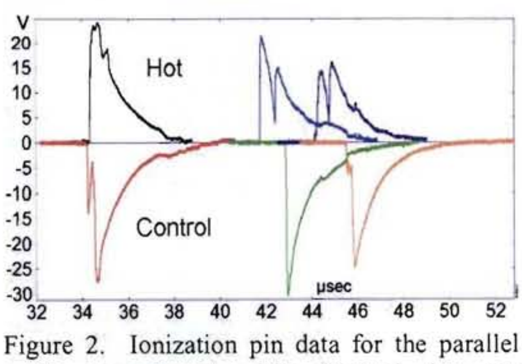

Figure 2. Ionization pin data for the parallel wedge experiment. The Control data are inverted to distinguish them from the Hot data.

The top of the figure shows the ionization pin data on the Hot wedge which was connected to the capacitor. The bottom shows the pin data for the shorted Control wedge. It can be seen that the ionization pin signals on the Hot side ran ahead of the Control data. The pin signals for the two wedges occurred at the same time at the thickest end of the wedges, but the Hot signals ran further and further ahead as the detonation progressed into the thinner regions. The peak voltage and current were 8 kV and 100 kA, the maximum electrical power deposited was 500 MW.

Similarly, the witness block data (not shown here) only showed differences for the 18-kV experiment. The dent for the Hot side ran ahead of the Control side by ~16 mm, although the edges of the dents were irregular making precise measurement difficult. The corresponding failure thicknesses were 2.9 and 2.1 mm; the temperature was 23°C; these are close to the AWE observations. Note that the wedges were confined on one side by the stainless steel witness block, so these are *confined* failure thicknesses. (The *unconfined* failure thickness of PBX-9502 at 20°C was 3.5 mm with a 2° wedge angle.[22])

Conclusions for Parallel Wedge Experiments

The results confirmed the AWE findings. In particular, Salisbury and Winter observed that there was a reduction in failure thickness above a critical capacitor voltage. Here too, with the parallel wedge experiments, there was no observable effect at the lower voltages. However, in the experiment perform at the highest voltage there were clear differences in the failure thickness. The reason why a minimum applied voltage appears to be necessary is not known.

Experiments in Magnetic Fields

Modified Gap Test in a Magnetic Field

Modified Gap Test (MGT) experiments were performed in a relatively large (1-T) magnetic field,[23] and the effects on surface velocities were observed with a DRS Imacon 200 image intensifier framing camera[24] and Photon Doppler Velocimetry gauges (PDV).[10] Surface velocities are a measure of the degree of reaction in the explosive. The camera had typical interframe times of 1 to 2 μs and an exposure time of 5 to 20 ns. Apart from the magnetic field the MGT test was identical to the original test,[25] using an unmodified 50.8-mm diameter by 12.7-mm thick acceptor charge of the same *cast-cured* HMX-based explosive used by Lee.[11] (Note that PBX-9501 is an HMX-based *pressed* explosive.)

The quasi-static magnetic fields were generated by pulsed 356-mm inside diameter Helmholtz coil pairs with a sinusoidal ¼-period of 125 μs; the experiments were synchronized to coincide with the peak of the fields so that they varied by less than 1% during the course of an experiment. Experiments were performed in pairs: one experiment with a particular gap thickness and no magnetic field; the other a repeat but with a magnetic field.

MGT Camera Results and PDV Data

No significant magnetic effects were observed in the MGT response of the HMX-based explosive in 18 tests. Despite careful quality control of the explosive manufacture the shock sensitivity of the HMX-based explosive varied more from experiment to experiment than it did due to the presence or absence of the magnetic field, as was also observed by Lee.[13] Consequently, the experiments with a magnetic field were inconclusive; the tests neither proved nor disproved the existence of a magnetic-field effect. However, if any magnetic effects existed they were small.

Higher initial velocities

The maximum velocity that could be measured with the PDV was limited by the electronic bandwidth of the digitizing oscilloscopes to ~8 km/s. In all tests, significantly higher *initial* surface velocities were observed with the PDV than could be detected with the Imacon. For example, in Figure 3 the peak PDV velocity ≥ 8 km/s and decayed to 4.5 km/s in ~1 μs; the velocity measured with the Imacon was also 4.5 km/s but due to the interframe time being 1 μs the initial peak velocity could not be detected. Again, the peak velocity was unaffected by the presence of a magnetic field.

Studies of Plasma Propagation in Air

Experiments were performed to observe the propagation of explosively generated plasma in air-filled tubes. They were performed with and without electric or magnetic fields and were

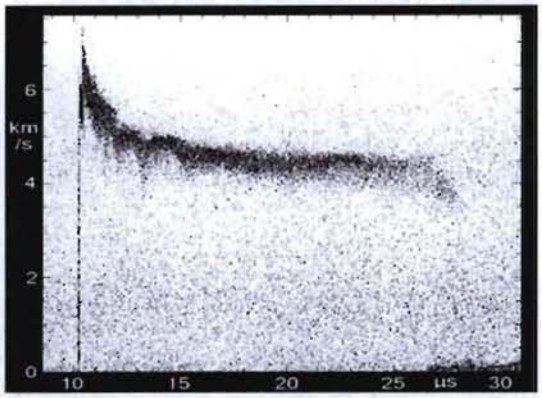

Figure 3. Spectrogram of PDV surface velocities in the MGT gap test experiment. Scales: km/s and μs.

observed with optical framing cameras, flash X-ray, and proton radiography diagnostics.

Plasma in Electric and Magnetic Fields

In both the electric and magnetic experiments the PBX-9501 explosive charges were 35 mm in diameter and 58 mm long, pressed into cylinders.[23] Each charge was detonator-initiated at one end and the plasma was observed at the other end. The surfaces of the charges were either bare or attached to 22-mm inside diameter straight plastic tubes, 150 mm in length. Plasma progress was monitored with an Imacon 200 framing camera[24] and metal witness blocks were used to detect differences in plasma formation.

Results: Plasma in magnetic fields

In the 17 experiments performed, the plasma *final* velocities, typically >8 km/s, were unaffected by the transverse 1-T magnetic fields and no differences were observed on the witness blocks. In terms of standard errors (σ) of the measured velocities, the velocity differences were up to 2.68σ between identical shots in zero fields. Between a field and no field the largest velocity difference was 2.91σ. From experiment to experiment the velocities in the magnetic fields were either higher or *lower* than in the zero field cases. In other words, no significant change in the final velocities could be detected that was caused by the magnetic fields.

However, there was evidence of higher *initial* velocities but it was too difficult to measure these accurately with the framing camera.

Opposing plasma in a magnetic field

In one experiment two plasma were fired towards each other, inside a straight horizontal plastic tube, Figure 4. A transverse magnetic field was applied in the direction of the camera axis so that the $\mathbf{v} \times \mathbf{B}$ forces were up and down in the figure. The measured plasma velocities were +8.34 and -8.41 km/s ± 0.06 km/s and thus agreed to within 1.15σ. The plasma shapes did not change with time and no helical paths were observed.

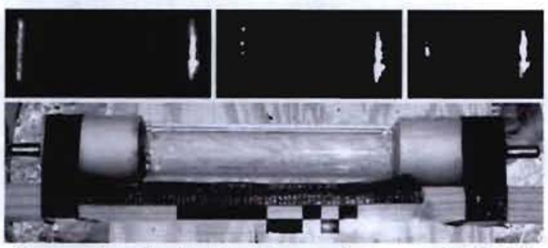

Figure 4. Explosive plasma in magnetic field. Top: Three frames at 1-μs intervals show the plasma progress. Bottom: opposing explosive charges separated by a plastic tube. The magnetic field was normal to the image.

Plasma in electric fields

With the same configuration and explosives as the magnetic experiments above, plasma were projected into 22-mm inside diameter straight plastic tubes and the progress was monitored with an Imacon 200 framing camera.

The electric field was applied between an aluminum mesh stretched across the top of the tube and a metal witness block at the other end. A 3 mm thick aluminum ring with a 20 mm inner diameter was attached to the mesh to maintain the electric field after the mesh had been destroyed by the plasma. Potential differences between the mesh and block were either plus or minus 60 kV.

As with the magnetic fields, no electrical effect was detected. In 20 experiments the plasma velocities were 8.4 ± 0.4 km/s and there was no correlation with the applied field, i.e., correlation coefficient ≈ 0.

Plasma Propagation Without Fields

Miniature plasma propagation studies in air

Plasma propagation experiments were studied on a small scale. In each experiment a 12.7-mm diameter, 12.7-mm long PBX-9501 pellet was placed on top of a polished acrylic block, Figure 5.

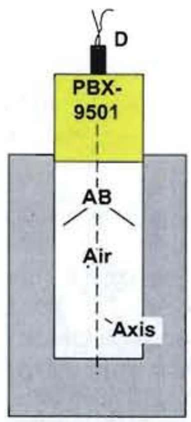

Figure 5. Schematic of small scale and pRAD plasma experiments. Key: D – detonator on axis; PBX-9501 – 12.7 mm diameter explosive cylinder; AB – polycarbonate or aluminum block. Not to scale.

The acrylic had an inside diameter of 12.7 mm, a cavity length of 25.4 mm and a wall thickness of 3.175 mm. The cavity contained air at ~78 kPa (at 2130 m altitude). The acrylic block was placed on top of an aluminum witness block.

The progress of the plasma was measured with optical and X-ray techniques. A 12-bit, 1280 x 1024 pixel, HSFC Pro Cooke image intensified camera[26] was used that produced eight frame images, each with an exposure time of 20 ns, a gain of 20%, and an interframe time of 200 ns. Four 150-kV Titon flash X-ray heads were arranged in a 90°/30° configuration to simultaneously observe the plasma.

The camera results revealed in every instance a thin bright luminous front travelling at 8.3 ± 0.4 km/s as in the top of Figure 6. The camera image has been pseudo-colored to reveal structure in the 12-bit digital image, as shown in the bottom of the figure. This shows that material, plasma or ejecta, travelled ahead and behind the

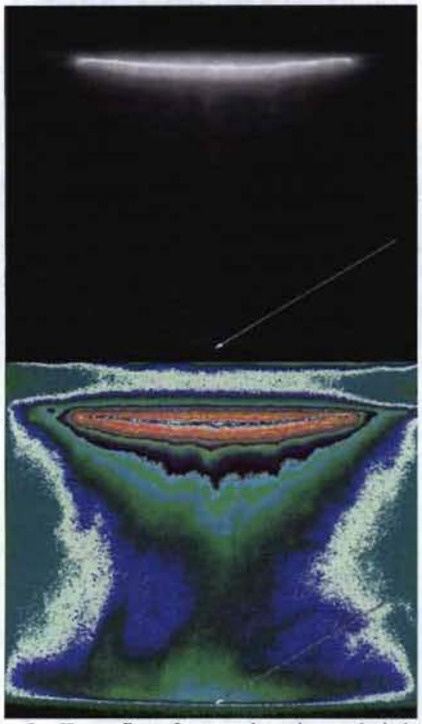

Figure 6. Top: first frame showing a bright line travelling downward in the cavity. Bottom: the same image processed in pseudo-color to reveal the 12-bit structure. The arrows indicate the bottom of the cavity.

bright line. In particular, the arrival of material was observed in the first frame at the bottom of the cavity after the detonation shock has emerged from the lower explosive surface; this occurred in all experiments.

Presumably, either material travelled ahead of the front and/or that some ionization event occurred caused by the reflection of detonation light at the bottom. In subsequent frames there appeared to be an accumulation of this material as the region increased in size and brightness.

The X-ray images, not shown, revealed that the region of greatest density was coincident with the bright luminous line. The apparent accumulation of material could not be resolved.

Proton Radiography (pRAD)

Experiments were performed to measure plasma densities and velocities using the 800-MeV proton radiation (pRAD) facility at the Los Alamos Neutron Science Center;[9] the general arrangement is the same as in Figure 5. A cylindrical detonating charge of PBX-9501, 12.7 mm in diameter and 12.7 mm long, projected plasma into an aluminum block with an air-filled cylindrical cavity. The complete assembly was surrounded by a vacuum. The progress of the experiment was monitored with the proton beam perpendicular to the cylinder axis.

With the pRAD imagery it was possible to produce line scans of image density versus position for dozens of images per experiment, thus building detailed records of the detonation wave propagation, Figure 7.

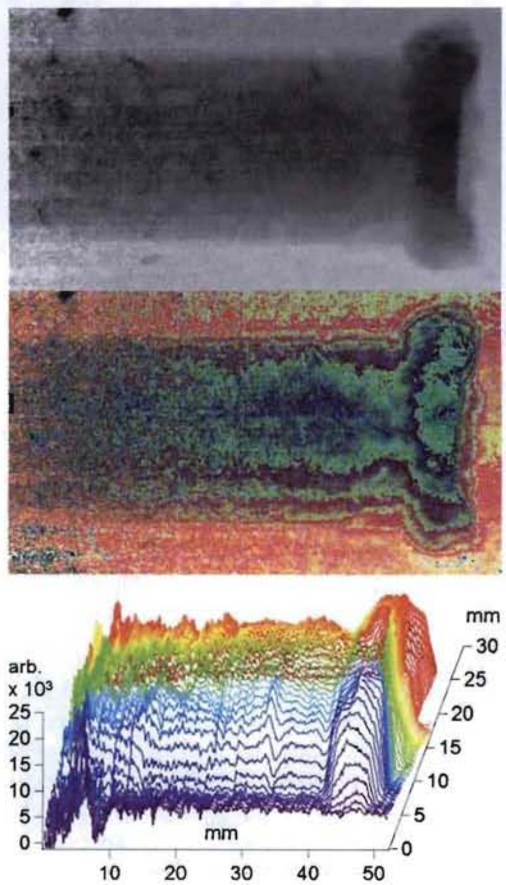

Figure 7. pRAD imagery. Top: raw image, detonation from the left, plasma impact with cavity bottom on the right. Middle: pseudo-color rendition of top image. Bottom: 3-D line scan rendition; the heights of the lines are in arbitrary units; the spacial dimensions in mm.

Unfortunately, the plasma were not visible in the pRAD images at any stage, although their impact at the bottom of the cylindrical cavities could be detected by deformation of material.

The pRAD image in Figure 7 is just one frame from one experiment but has been chosen as it is representative of all the data. The plasma could not be detected in the cavity, even with the aid of pseudo-colorization and line plots. However, the plasma interaction with the base of the cavity is clearly visible. Animations made from multiple frames show that the plasma formed a toroidal vortex as it travelled down the cavity, rolling down the walls. The direction of the rotation in the bottom right hand corner of the figure was clockwise.

Summary and Discussion

Possible explanations for the observed *electric field* effects include: bulk heating of the reaction products by Joule heating; reduction of the energy barrier that facilitates dislocation motion, perturbations to the activation energy for chemical reaction, and acceleration of plasma projected from the reaction zone.

Bulk Joule heating of the reaction products can enhance the reactivity of the explosives[27-29] but is not a likely explanation for most of the observed effects. That is because for quantifiable effects to be observed the necessary electrical powers must be of the same order as the chemical power liberated by reaction. The detonation power density, i.e., the chemical power liberated by a detonating high explosive per unit area is $P_{\text{det}} = \rho_0 D Q_{\text{det}}$ where ρ_0 is the density, D the detonation velocity and Q_{det} the heat of detonation. $P_{det} \approx 100\ \text{TW/m}^2$for a typical high explosive. With the possible exception of the LANL-wedge experiments (Figure 1) which deposited an estimated peak power density of $10\ \text{TW/m}^2$ the power densities were significantly smaller. So bulk Joule heating is an unlikely explanation for the other experiments.

Coffey[1] suggested the possible perturbation of the Peierls energy barrier by an applied electric field which would facilitate dislocation motion. This process might be more pertinent to the initiation and growth of reaction and could account for the electric effects observed by both Cook and Lee. It is unlikely to account for the effects on full detonation observed by AWE and reported here.

In all instances the explosives were inhomogeneous, thus containing randomly oriented explosive crystals. Consequently, only a fraction of the crystals would be aligned with the direction of the electric field. Therefore the field should lower the energy barrier and facilitate dislocation motion in some crystals and restrict motion in others.

Similarly, in the case of perturbations to the activation energy for chemical reaction, it is difficult to explain how such an effect would apply to randomly oriented crystals.

In this work we have focused on the possible role of plasma ejected from detonating explosives. It is clear that there is still much to learn about the role of plasma. Data from a variety of experiments have been compared to determine the nature of plasma ejected from detonating explosives and their possible role in the initiation and growth of reaction. If plasma contribute to initiation and growth then electromagnetic fields should affect their contributions.

Electric and magnetic field effects on initiation and growth have been reported previously. In this work we were able to replicate the electrical effects on wedges of TATB-based but could not detect electric or magnetic effects, on HMX-based explosives. The failure to detect these effects could be due the fact that none exist or due to the lower electrical conductivity of detonating HMX compared to the Dithekite 13 and TATB. It is known that the explosive product conductivity of TATB-based PBX-9502 is 5000 S/m compared to PBX-9501 (300 S/m).[27] The electrical conductivity of detonating Dithekite 13 is estimated to be ~1300 S/m using the correlation of conductivity with percentage carbon in the products[30] and a calculation of the carbon content.[31] (Cook[12] studied the effects of electric fields on Comp-B, which has a conductivity of 1200 S/m.) Consequently, the experiments reported here on PBX-9501 may have shown no effects of electromagnetic fields because the conductivity of the plasma was too low. As shown, the magnetic field cannot change the kinetic energy of a charged particle, so no magnetic effects on plasma velocity would be expected. The Lorentz forces of a parallel magnetic field could reduce the divergence of the ejecta from a detonating surface giving an apparent increase in velocity, i.e., by focusing the ejecta.

The framing camera images from miniature plasma experiments showed something travelling ahead of the bright plasma and reaching the cavity bottom within the first frame. This was either plasma or some ionization event caused by the reflection of detonation light at the bottom or an electrical effect.[7] Subsequent frames showed an accumulation of this material as the region increased in size and brightness. The mass-velocity distribution of any impacting ejecta could be studied with the Asay thick plate or similar technique[32]

To conclude, no electric or magnetic field effects on plasma have been detected that would support the hypothesis that they contribute either to the reaction and growth or detonation of explosives. However, the HMX-based explosives used here may have been less sensitive to electromagnetic fields than other explosives because of their low electrical conductivity.

Acknowledgement

This work was funded in part by the US Defense Threat Reduction Agency (DTRA) for which the authors are most grateful. They also acknowledge many helpful discussions with Dr. C. Boswell, NSWC Indian Head; and thank Dennis Herrera, David Torres, John Echave, Steven Hare, Matthew Briggs, and Michael Shinas (all from LANL) for their experimental assistance. We also gratefully thank the LANL pRAD team.

References

1. Coffey, C.S., "Quantum-mechanical aspects of dislocation motion and plastic flow," Physical Review B, 1994. 49(1): p. 208.

2. Cook, M.A., The Science of High Explosives. 1958, New York: Reinhold Publishing Co.

3. Cook, M.A. and McEwan, W.S., "Cohesion in Plasma," J. Appl. Phys., 1958. 29(11): p. 1612-1613.

4. Bauer, A., Cook, M.A., and Keyes, R.T., "Detonation-Generated Plasmas," Proc. Roy. Soc. Series A, 1961. 259(1299): p. 508-517.

5. Davis, W.C. and Campbell, A.W., "Ultra-High-Speed Photographs Refuting ``Cohesion in Plasma"," J. Appl. Phys., 1960. 31(7): p. 1225-1227.

6. Fortov, V.E., Musyankov, S.I., Yakushe, V.V., and Dremin, A.N., "Anomalous Effects In The Appearance Of A Detonation Wave At A Free Surface," Teplofizika Vysokikh Temperatur, 1974. 12(5): p. 7.

7. Boswell, C.J. and O'Connor, P.D., "Charged Particle Motion in an Explosively Generated Ionizing Shock," in Shock Compression of Condensed Matter - 2009 (M.D. Furnish, eds.), pp. 400-403.

8. Spaulding, R.L., Jr., "Precursors in Detonations in Porous Explosives," in Seventh Symposium (International) on Detonation - 1981 (J.M. Short and S.J. Jacobs, eds.), pp. 877-886.

9. Mottershead, T., Barlow, D., Blind, B., Hogan, G., et al., "Design and Operation of a Proton Microscope for Radiography at 800MeV," in 2003 Particle Accelerator Conference. 2003. Portland, OR, USA.

10. Strand, O.T., Goosman, D.R., Martinez, C., Whitworth, T.L., et al., "Compact system for high-speed velocimetry using heterodyne techniques," Rev. Sci. Inst., 2006. 77(8): p. 083108-8.

11. Lee, R.J., Forbes, J.W., Palermo, E., and Wilson, W.H., "Effect of electric fields on sensitivity of an HMX based explosive," in Shock Compression of Condensed Matter - 2007 (M. Elert, et al., eds.), pp. 963-966.

12. Cook, M.A. and Gwyther, T.Z., "Influence of Electric Fields on Shock to Detonation Transition." 1965, Utah University: Salt Lake City, UT, USA.

13. Lee, R.J., Forbes, J.W., Tasker, D.G., and Orme, R.S., "Changes In Blow-Off-Velocity Observed In Two Explosives At The Threshold

For Sustained Ignition Using The Modified Gap Test," in Shock Compression of Condensed Matter - 2009 (M.D. Furnish, eds.).

14. Salisbury, D., Winter, R., and Biddle, L., "A Study Of The Effect Of Electrical Energy Input On Detonation Failure In Wedges Of The TATB-Based Explosive EDC35," in Shock Compression of Condensed Matter - 2005 (M.D. Furnish, et al., eds.), pp. 1010-1013.

15. Winter, R.E., Salisbury, D.A., Biddle, L., and James, H.R., "The Effect Of Electrical Energy On Detonation Failure In Wedges Of The TATB-Based Explosive EDC35," in Thirteenth International Detonation Symposium - 2006 (S. Peiris and R. Doherty, eds.), pp. 52-62.

16. Cook, M.A., Keyes, R.T., and Udy, L.L., "Propagation Characteristics of Detonation-Generated Plasmas," J. Appl. Phys., 1959. 30(12): p. 1881-1892.

17. Sheffield, S., Alcon, R., Gustavsen, R., Graham, R., et al., "Particle velocity and stress measurements in low density HMX," in High Pressure Science and Technology - 1993 (S.C. Schmidt, et al., eds.), pp. 1377.

18. Tasker, D.G., "The Properties of Condensed Explosives for Electromagnetic Energy Coupling." 1985, Naval Surface Warfare Center: White Oak, MD, USA.

19. Tasker, D.G., Lee, R.J., and Gustavson, P.K., "An Explosively-Actuated Electrical Switch Using Kapton Insulation." 1992, Naval Surface Warfare Center: White Oak, MD, USA.

20. Pearson, 411 current transformer. Available from: http://www.pearsonelectronics.com/.

21. Beverly III, R.E. and Campbell, R.N., "Aqueous-electrolyte resistors for pulsed power applications," Rev. Sci. Inst., 1995. 66(12): p. 5625-5629.

22. Ramsay, J.B., "Effect of confinement on failure in 95 TATB/5 Kel-F.," in Eighth Symposium (International) on Detonation - 1985 (J.M. Short and W.E. Deal, eds.), pp. 372-379.

23. Tasker, D.G., "Electromagnetic field effects in explosives," in Shock Compression of Condensed Matter - 2009 (M.D. Furnish, eds.).

24. Itronx, Imacon 200. 2009; Available from: http://www.itronx.com/DRS_IMACON_200%20_high-speed_slow-motion_cameras.htm.

25. Liddiard, T.P., Jr and Jacobs, S.J., "Initiation of Reaction in Explosives and Propellants." 1965, Naval Ordnance Laboratory: White Oak, Silver Spring, MD.

26. Cooke, hsfc-pro Intensified Camera. Available from: http://www.cookecorp.com/intensified-cameras/hsfc-pro/.

27. Tasker, D.G. and Lee, R.J., "The Measurement of Electrical Conductivity in Detonating Condensed Explosives," in Ninth Symposium (International) On Detonation 1989. Portland, OR, USA.

28. Lee, J., Kuk, J.-H., Kim, C.-H., and Hwang, E.-H., "Enhancement Of Detonation Properties By Electric Energy Input," in APS Topical Conference on Shock Compression of Condensed Matter - 1999 (M.D. Furnish, L.C. Chhabildas, and R.S. Hixson, eds.), pp. 865-868.

29. Tasker, D.G., "Electromagnetic Energy Coupling in Condensed Explosives." 1989, Naval Surface Warfare Center: White Oak, MD, USA.

30. Hayes, B., "On Electrical Conductivity in Detonation Products," in Fourth Symposium (International) on Detonation. 1965.

31. Bastea, S., Fried, L.E., Glaesemann, K.R., Howard, W.M., et al., "Cheetah 5.0." 2007, Energetic Materials Center, Lawrence Livermore National Laboratory: Livermore, CA. p. A thermochemical code.

32. Asay, J.R., "Thick-plate technique for measuring ejecta from shocked surfaces," J. Appl. Phys., 1978. 49(12): p. 6173-6175.